A Novel Fluorinated Metal-organic Framework for Xenon/Krypton Separation[①]

WU Xiao-Ling[a]   LI Zi-Jian[a]   TANG Fang-Dong[b]

QIAN Nan[a]   CHU Xin-Xin[a②]   LIU Wei[a②]

[a] (*Shanghai Institute of Applied Physics, Chinese Academy of Science, Shanghai* 201800, *China*)

[b] (*Shanghai Institute of Measurement and Testing Technology, Shanghai* 201203, *China*)

ABSTRACT   A porous metal-organic framework $[C_{21}H_{20}CoF_6O_7]$ was synthesized with $Co(CH_3COO)_2$ $4H_2O$ and CPHFP (2,2′-bis(4-carboxyphenyl)hexafluoro-propane) under hydrothermal conditions. This FMOF-Co has been characterized by elemental analysis, infrared spectroscopy, thermogravimetric analysis, single-crystal and powder X-ray diffraction. The crystal is of monoclinic space group $P2_1/n$ with a = 7.8911(2), b = 29.9053(8), c = 10.5811(3) Å, β = 90.193(10)°, V = 2499.70(12) Å^3, Z = 4, M_r = 557.3, D_c = 1.481 g cm^{-3}, $F(000)$ = 1132, μ = 0.768 mm^{-1}, $GOOF$ = 1.035, the final R = 0.0722 and wR = 0.2326 for 6347 observed reflections with $I > 2\sigma(I)$. The structure of FMOF-Co is constructed form the linkage of Co(II) through CPHFP, forming a 3D net framework. The Kr and Xe uptake values are 0.225 and 0.484 mmol g^{-1} at 303 K (100 KPa) with their mol selectivity to be 0.46; while the Kr and Xe uptake values are 0.486 and 0.077 mmol g^{-1} at 233 K (100 KPa), with their mol separation being 6.29 at this condition.

Keywords: fluorinated MOFs, crystal structure, gas adsorption; DOI: 10.14102/j.cnki.0254–5861.2011–2776

1   INTRODUCTION

Effluent gas containing Xe and Kr atoms from nuclear fuel reprocessing plants is the main problem of the environment pollution, which should be treated and captured in an efficient way. ^{85}Kr, as a radioactive element with a half-life of 10.3 years, may influence climate and human health, triggering some potential genetic diseases[1]. Moreover, the separation and storage of Kr are highly necessary and worthwhile to industry and medical applications like imaging, anesthesia as well as lighting in traffic systems[2]. Recently, the commercial development of ^{85}Kr capture with cryogenic distillation is limited since its high energy and cost[3, 4]. The pressure swing method is usually applied in the radioactive gases' treatment for most nuclear plants via the activated charcoal fixed bed, which is not efficient for Xe and Kr separation. Therefore, materials with advanced pore structure

have been chosen as prospective alternatives for the separation of Xe/Kr mixtures[5].

Metal-organic frameworks (MOFs) are defined as porous materials being comprised of metal clusters and organic ligands[6]. Due to the various chemical functionalities attached, well-defined pore size, large surface area as well as high porosity, MOFs can be utilized in specific application, especially in gas separation and catalysis process[7]. Currently, most studies are focusing on the green-house gas separation such as CH_4, CO_2 as well as hydrocarbon capture with MOFs in post-combustion processing[8, 9]. Studies on Xe/Kr separation are meaningful and urgent for the treatment of radioactive effluent gases from nuclear power plant.

Many researchers concentrated on the separation of Xe and Kr at room temperature, such as Debasisi Banerjee et al. confirmed that SB-MOF has high selectivity with Henry coefficient 16.21 at 298 K[10]. Thallapally and co-workers

demonstrated that the Ni-DOBDC has higher separation coefficient in Xe/Kr selectivity than active carbon and HKUST[11, 12], while few studies experimented the Xe and Kr in different temperature.

Herein fluorinated metal-organic framework (FMOFs), a novel type of porous materials with advanced thermal stability and low surface tension, is selected[13, 14]. Moreover, not many available publications focused on MOFs with fluorinated ligands[15], and therefore CPHFP (2,2′-bis(4-carboxyphenyl)hexafluoro-propane) is chosen as the organic ligand which is flexible and shown to provide some breathing phenomena in the solid state[16-18]. Light pink crystal was obtained through the coordination of CPHFP as organic ligand with cobalt metal, constructing a chemo-stable microporous framework FMOF-Co. Single-crystal structural analysis reveals that FMOF-Co features rhombus network topology based on the Co(II) clusters as connected nodes and CPHFP as connected ligands. Measurements of Kr and Xe uptake were conducted to show the high separation coefficient of Kr of FMOF-Co under low temperature.

2   EXPERIMENTAL

2. 1   Materials and instruments

All chemicals were purchased from commercial sources and used without further purifications. C and H were tested on an ELEMENTAL Vario cube analyzer for elemental analysis (EA). Sample was measured through the infrared (IR) spectra (Thermo NICOLET IS5) in the range of $500\sim4000$ cm^{-1}. Powder X-ray diffraction (PXRD) data were collected on a Bruker Advance D8 with Cu$K\alpha$ radiation and diffractometer with a scan speed of 2 $°\cdot min^{-1}$. NETSCHZ STA-449C was utilized for thermogravimetric analysis (TGA) under Ar (range $25\sim900$ °C) at a heating rate of 10 °C min^{-1}. The gases adsorption isotherms were recorded by utilizing micromeritic ASAP-2020 volumetric adsorption equipment (using N_2, He, Xe and Kr of ultrahigh purity grade, >99.999%).

2. 2   Synthesis of FMOF-Co

A mixture of CPHFP (2,2′-bis(4-carboxyphenyl)hexa-fluoro-propane) (120 mg, 0.3 mmol) and $Co(CH_3COO)_2\cdot4H_2O$ (75 mg, 0.3 mmol) was dissolved in 2 mL solution (ethanol/H_2O, v/v 1:1), then the mixture was transferred into a 10 mL Teflon-lined stainless-steel vessel, and kept at 80 °C for 3 days. After cooling down to room temperature, block light pink crystals were obtained with the

yield of 60% based on CPHFP (2,2′-bis(4-carboxyphenyl) hexafluoro-propane). FT-IR ($4000\sim400$ cm^{-1}): 3230(m), 1590(m), 1540(m), 1380(m), 1240(m), 1210(m), 1170(m), 1020(m), 930(m), 782(m), 746(m), 722(s), 491(m), 450(m). EA calcd. ($C_{21}H_{20}CoF_6O_7$): C, 45.24; H, 3.59%. Found: C, 42.45; H, 2.93%. Volatile guest solvents could lead to the difference between calculated and measured EA values. Before the adsorption experiment, samples were washed with ethanol to remove the water and unreacted organic ligands and then immersed in n-hexane for 6 h.

2. 3   Structure determination

A light pink monoclinic crystal of FMOF-Co (0.30mm × 0.10mm × 0.08mm) was chosen and placed in the sample clap. Single-crystal X-ray diffraction (SCXRD) data were recorded on Bruker Advanced D8-Venture with Mo$K\alpha$ radiation (λ = 0.71073 Å) at 77 K. A total of 21428 reflections were collected at 77 K in the range of $2.36\leqslant\theta\leqslant28.77$ °by using an ω-scan mode, and 9845 were received with R_{int} = 0.0305 and 6347 were observed with I > $2\sigma(I)$. The structure was solved by direct methods with OLEX2 and refined by full-matrix least-squares methods with SHELXL-2016 program package[19]. The final R = 0.0722, wR = 0.2326 ($w = 1/[\sigma^2(F_o^2) + (0.1427P)^2 + 5.3932P]$, where $P = (F_o^2 + 2F_c^2)/3$), S = 1.064, $(\Delta/\sigma)_{max}$ = 0.001, $(\Delta\rho)_{max}$ = 2.158 and $(\Delta\rho)_{min}$ = −1.506 e Å^{-3}. Selected bond lengths and bond angles from X-ray structure analysis are listed in Table 1.

3   RESULTS AND DISCUSSION

3. 1   Crystal structure description

Crystal structural analysis showed that FMOF-Co is in the monoclinic space group $P2_1/n$, which revealed the coordination environments around Co^{2+} ions (Fig. 1a). In each asymmetric unit, there is one Co^{2+} ion bridged with two coordinated ethanol molecules and two CPHFP links. Ligand CPHFP is deprotonated during the self-assembly reaction. Co(1) adopts six-coordinated modes: Co(1) links to two μ_2-aqua oxygen atoms, two carboxy oxygen atoms from two CPHFP links and two carboxy oxygen atoms from CH_3CH_2OH molecule. The bond angle of Co(1)–(μ_2–O)–Co(2) is 127.18 °. The distance between Co(1) and Co(2) is 3.95 Å and that between Co(1b) and Co(2) is 15.861 Å. All the bond lengths of Co–O are in the range from 2.024 to 2.205 Å. Each Co^{2+} ion connects four neighboring Co^{2+} ions through CPHFP (2,2′-bis(4-carboxyphenyl)hexafluoro-pro-

pane) ligands, leading to a two-dimensional (2D) (4,4)-gird-typed layer (Fig. 1b). Theses sheets are connected with each other through the μ_2-aqua oxygen atoms to form a 3D framework with rhombic shaped channel suitable for Xe and Kr adsorption. Two CH_3CH_2O groups are connected with Co(1), which plays a role as sieve, so only gases with suitable size can enter the hole.

(a)　　　　　　　　　　　　**(b)**
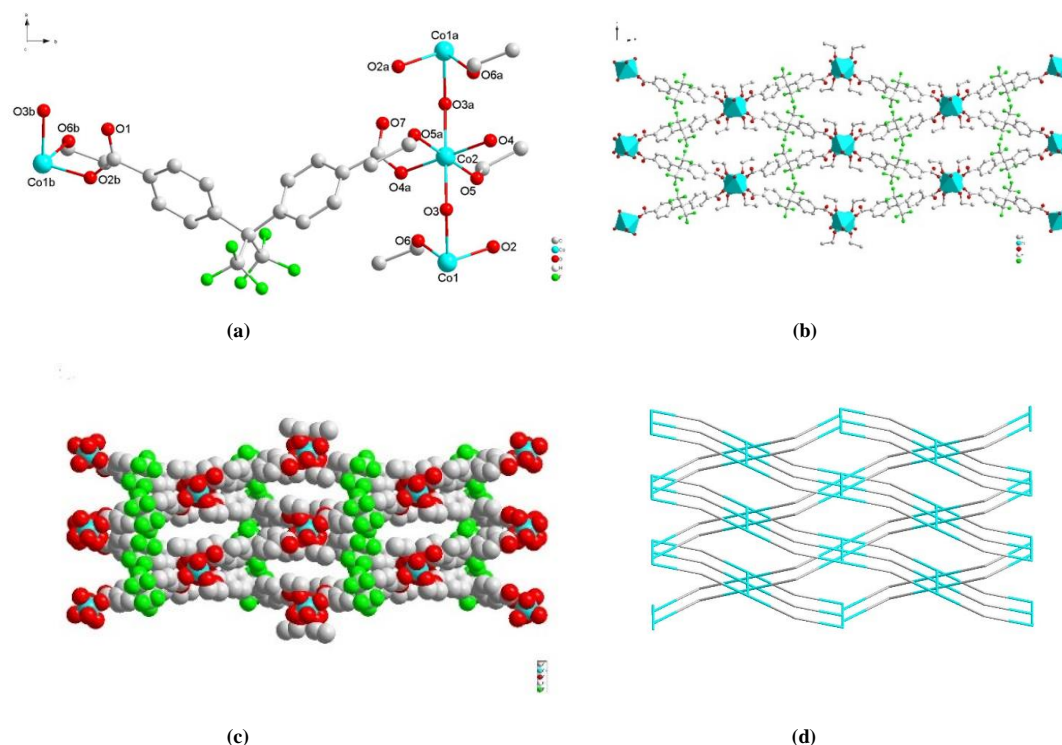

(c)　　　　　　　　　　　　**(d)**

Fig. 1.　(a) Local coordination environment (symmetry codes: a: –x–1/2, –y+1/2, –z+2; b: x, –y+1, z–1/2;
(b) FMOF-Co grid-like layer, (c) Packing diagram by space-filling model, and (d) Topological net of FMOF-Co

Table 1.　Selected Bond Lengths (Å) and Bond Angles (°)

Bond	Dist.	Bond	Dist.	Bond	Dist.
Co(1)–O(3)	2.205	Co(1)[a]–O(3)[a]	2.205	Co(2)–O(4)	2.024
Co(1)–O(2)	2.024	Co(1)[a]–O(6)[a]	2.065	Co(2)–O(4)[a]	2.024
Co(1)–O(6)	2.065	Co(2)–O(3)[a]	2.205	Co(2)–O(5)	2.059
Co(1)[a]–O(2)[a]	2.024	Co(2)–O(3)	2.205	Co(2)–O(5)[a]	2.059
Angle	(°)	Angle	(°)	Angle	(°)
O(6)–Co(1)–O(3)	88.735(1)	O(6)[b]–Co(1)[b]–O(2)[b]	89.769(1)	O(4)[a]–Co(2)–O(3)[a]	92.607(1)
O(6)–Co(1)–O(2)	90.231(1)	Co(1)–O(3)–Co(2)	127.18(1)	O(4)[a]–Co(2)–O(4)	180
O(2)[a]–Co(1)[a]–O(3)[a]	87.401(1)	Co(1)–O(3)[a]–Co(2)	127.18(1)	O(4)[a]–Co(2)–O(5)	90.492(1)
O(2)[a]–Co(1)[a]–O(6)[a]	90.231(1)	O(5)[a]–Co(2)–O(3)[a]	87.937(1)	O(4)[a]–Co(2)–O(3)	87.393(1)
O(3)–Co(1)–O(6)[a]	88.735(1)	O(5)[a]–Co(2)–O(4)	90.492(1)	O(3)[a]–Co(2)–O(3)	180
O(3)[a]–Co(1)–O(2)	87.401(1)	O(5)[a]–Co(2)–O(5)	180	O(3)[a]–Co(2)–O(4)	92.607(1)
O(6)[b]–Co(1)[b]–O(3)[b]	88.735(1)	O(5)[a]–Co(2)–O(3)	92.063(1)	O(3)[a]–Co(2)–O(5)	87.937(1)
O(3)[b]–Co(1)[b]–O(2)[b]	92.599(1)	O(5)[a]–Co(2)–O(4)[a]	89.508(1)		

Symmetry transformation: a: –x–1/2, –y+1/2, –z+2; b: x, –y+1, z–1/2; c: x, –y, z–1/2

3. 2　PXRD, TGA and chemostability

The PXRD test was used to test the purity of the crystal, confirmed with the simulation results from SCXRD test (Fig. 2a). The thermal stability was tested in temperature range of 25～900 °C by TGA measurement under Argon atmosphere (Fig. 2b). FMOF-Co lost 5% of its weight at 100 °C, which may be the departure of low-boiling solvent like ethanol, then it continued to lose 10% of its weight attributed to the loss of water molecule. A rather stable platform appeared from 200 to 450 °C. The construction of the product started to collapse at 450 °C and decomposed totally at 700 °C, indicating an excellent thermal stability in this

temperature range. No obvious changes in PXRD patterns of FMOF immersed in different solvents (e.g. methanol, ethanol, acetone, n-hexane, dichloromethane and *N,N*-dimethylfor-

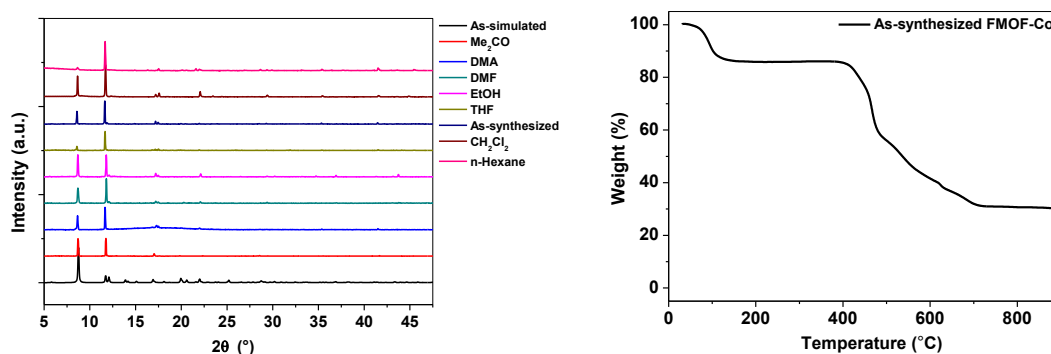mamide) for 24 h, manifesting a good chemical stability of FMOF-Co (Fig. 2a).

Fig. 2.　(a) PXRD patterns of FMOF-Co under different chemical conditions, (b) TGA curves of FMOF-Co

3. 3　Separation of Xe/Kr under different temperature

The crystal FMOF-Co was activated at 100 °C in high vacuum for 6 h and tested by the N_2 adsorption-desorption isotherm at 77 K. Fig. 3a shows a type-II reversible sorption behavior for microporous materials. Brunauer-Emmett-Teller (BET) surface area of FMOF-Co was tested to be 67.63 $m^2\ g^{-1}$ (Langmuir surface area: 130.46 $m^2\ g^{-1}$). Experiments were carried out from 233 to 303 K for the adsorption capacity and selectivity of Kr and Xe for FMOF-Co. As shown in Fig. 4b and 4c, the appreciable Kr trap at 303 K was found to be 0.225 mmol g^{-1} at 100 KPa. With the decrease of temperature, the uptake of Kr increased gradually and reached 0.49 mmol g^{-1} at 233 K. As for Xe, the amount of uptake was 0.48 mmol g^{-1} at 303 K (100 KPa). With the temperature decreased, Xe uptake capacity firstly increased

and achieved 0.58 mmol g^{-1} at 273 K, and then decreased to 0.08 mmol g^{-1} at 233 K. According to Fig. 5e, the mol selectivity of Kr/Xe was from 0.46 to 6.29, which means that the Kr and Xe separation can be controlled by varying the temperature of operation. In the temperature range of 253～303 K, FMOF-Co adsorbed more Xe than Kr. When the temperature decreased from 253 to 233 K, it adsorbed more Kr than Xe. This change in the amount of adsorption for Kr and Xe can be ascribed to the temperature-dependent gating effect. The larger Xe atoms cannot overcome the potential barriers enter the holes at low temperature due to its lower kinetic energy, while the interaction of smaller Kr atoms and adsorbent becomes stronger as the temperature decreases, and therefore the adsorption quantity is higher than Xe.
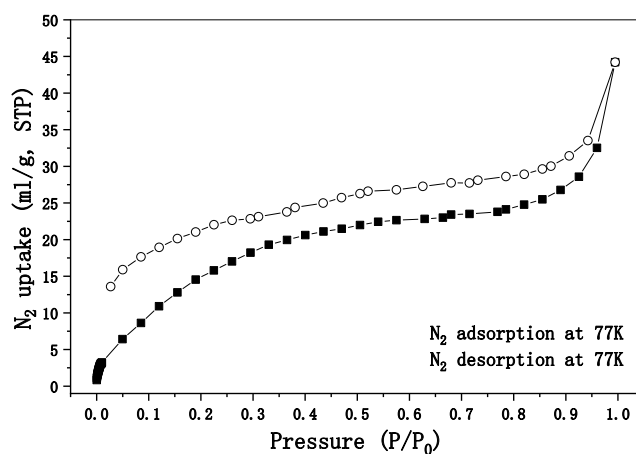

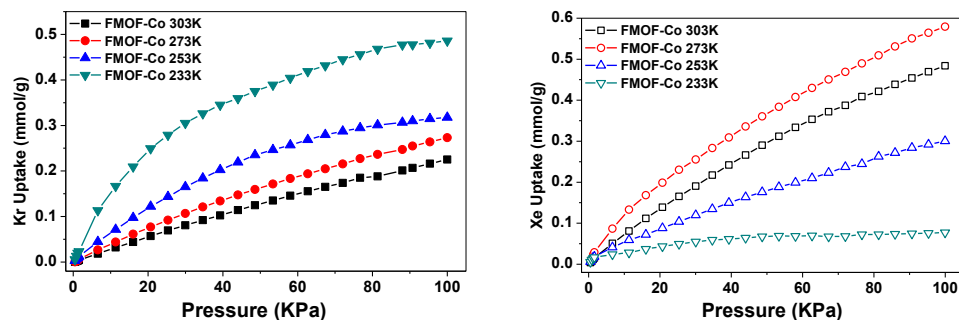Fig. 3.　(a) N_2 adsorption-desorption isotherm at 77 K

Fig. 4.   (b) Kr uptake capacity from 233 to 303 K, (c) Xe uptake capacity from 233 to 303 K
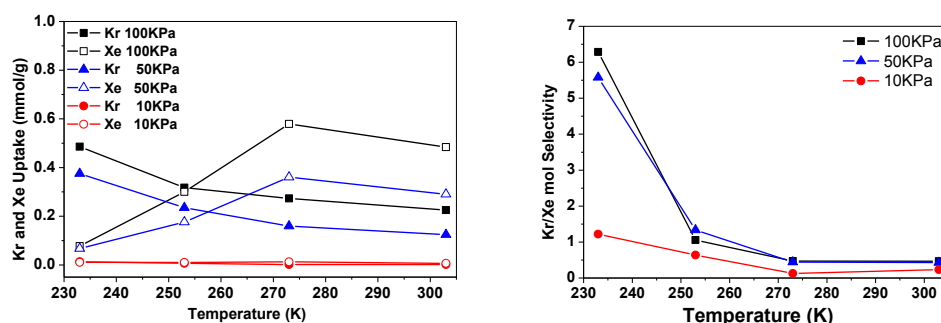

Fig. 5.   (d) Kr and Xe adsorption quantity at different pressure and temperature,
(e) Kr/Xe mol selectivity from 233 to 303 K with different pressure

4   CONCLUSION

In conclusion, a 3D metal-organic-framework of $[C_{21}H_{20}CoF_6O_7]$ FMOF-Co was synthesized under the solvothermal conditions and characterized by single-crystal X-ray diffraction. The XRD pattern revealed FMOF-Co consisted of grid-layers based on Co^{2+} and CPHFP (2,2′-bis(4-carboxyphenyl)hexafluoro-propane) ligands. With good thermal and chemical stability, the FMOF-Co also exhibited reversible Kr and Xe selectivity in different temperature ranges (303～233 K). Kr/Xe mol selectivity ranged from 0.46 to 6.29 at 100 KPa, indicating that the Xe and Kr selectivity can be controlled by adjusting temperature.

REFERENCES

(1)   Smith, K. R.; Frumkin, H.; Balakrishnan, K.; Butler, C. D.; Chafe, Z. A.; Fairlie, I.; Kinney, P.; Kjellstrom, T.; Mauzerall, D. L.; McKone, T. E.; McMichael, A. J.; Schneider, M. Energy and human health. *Annu. Rev. Public Health* **2013**, 34, 159–188.

(2)   Cullen, S. C.; Gross, E. G. The anesthetic properties of xenon in animals and human beings with additional observations on krypton. *Science* **1951**, 113, 580–582.

(3)   Izumi, J.; Auerbach, S. M.; Carrodo, K. A.; Dutta, P. K. Waste gas treatment using zeolites in nuclear-related industries. In: (Eds.). *Handbook of Zeolites Science and Technology*. Marcel Dekker: New York **2003**.

(4)   Kerry, F. G. *Industrial Gas Handbook: Gas Separation and Purification*; CRC Press: Boca Raton Florida **2007**.

(5)   Yang, R. T.; Adsorbents: fundamentals and Applications. John Wiley & Sons Inc.: Hoboken **2003**.

(6)   Rowsell, J. L. C.; Yaghi, O. M. Metal-organic frameworks: a new class of porous materials. *Micropor. Mesopor. Mater.* **2004**, 73, 3–14.

(7)   Férey, G. Hybrid porous solids: past, present, future. *Chem. Soc. Rev.* **2008**, 37, 191–214.

(8)   Bae, Y. S.; Snurr, R. Q. Development and evaluation of porous materials for carbon dioxide separation and capture. *Angew. Chem. Int. Ed.* **2011**, 50, 11586–11596.

(9)   Wang, M.; Zhuo, C.; He, L.; Lin, Q. P. Synthesis, crystal structure and gas adsorption of a trimeric nickel-based coordination polymer. *Chin. J. Struct. Chem.* **2019**, 38, 345–350.

(10) Banerjee, D.; Simon, C. M.; Plonka, A. M.; Motkuri, R. K.; Liu, J.; Chen, X.; Smit, B.; Parise, J. B.; Haranczyk, M.; Thallapally, P. K. Metal-organic framework with optimally selective xenon adsorption and separation. *Nature Communications*   **2016**,7,11831.

(11) Liu, J.; Thallapally, P. K.; Strachan, D. M. Metal-organic frameworks for removal of Xe and Kr from nuclear fuel reprocessing plants. *Langmuir.* **2012**, 28, 11584–11589.

(12) Thallapally, P. K.; Grate, J. W.; Motkuri, R. K. Facial xenon capture and release at room temperature using a metal-organic framework: a comparison with activated charcoal. *Chem. Commun.* **2012**, 48, 347–349.

(13) Yang, C.; Wang, X. P.; Omary, M. A. Fluorous metal-organic frameworks for high-density gas adsorption. *J. Am. Chem. Soc.* **2007**, 129, 15454–15455.

(14) Fernandez, C. A.; Thallapally, P. K.; Motkuri, R. K.; Nune, S. K.; Sumrak, J. C.; Liu, J. Gas-induced expansion and contraction of a fluorinated netak-organic framework. *Cryst. Growth Des*. **2010**, 10, 1037–1039.

(15) Liu, Z. Q.; Stren, C. L.; Lambert, J. B. Metal-organic frameworks from dipodal and tripodal silicon-centered tetrahedral ligands. *Organometallics* **2009**, 28, 84–93.

(16) Thallapally, P. K.; Tian, J.; Kishan, M. R.; Fernandez, C. A.; Dalgarno, S. J.; McGrail, P. B.; Warren, J. E.; Atwood, J. L. Flexible (breathing) interpenetrated metal-organic frameworks for CO_2 separation applications. *J. Am. Chem. Soc.* **2008**, 130, 16842–16843.

(17) Thallapally, P. K.; McGrail, B. P.; McGrail, P. B.; Dalgarno, S. J.; Atwood, J. L. Gas/solvent-induced transformation and expansion of a nonporous solid to 1:1 host guest form. *Cryst. Growth Des*. **2008**, 8, 2090–2092.

(18) Fernandez, C. A.; Liu, J.; Thallapally, P. K.; Strachan, D. M. Switching Kr/Xe selectivity with temperature in a metal-organic framework. *J. Am. Chem. Soc.* **2012***, 134, 9046–9049.

(19) Sheldrick, G. M. *SHELXS-97 and SHELXL-97, Program for X-ray Crystal Structures Solution and Refinement.* University of Göttingen, Germany **1997**.